

International Conference on Advances Science and Contemporary Engineering 2012
(ICASCE 2012)

Kinematic and Aerodynamic Modelling of Flapping Wing Ornithopter

Harijono Djojodihardjo^{a*}, Alif Syamim Syazwan Ramli^b and Surjatin
Wiriadidjaja^c

^aProfessor, ^bGraduate Student, ^cAssociate Professor
*Department of Aerospace Engineering, Faculty of Engineering, Universiti Putra Malaysia
43400 UPM SERDANG, Selangor, Malaysia*

Abstract

A generic approach is carried out to model the kinematics and aerodynamics of ornithopter to mimic flapping wing to produce lift and thrust for hovering and forward flight, by considering the motion of a three-dimensional rigid thin wing in flapping and pitching motion with phase lag. Basic Unsteady Aerodynamic Approach incorporating salient features of viscous effect and leading-edge suction will be utilized. Parametric study is carried out to reveal the aerodynamic characteristics of ornithopter flight characteristics and for the analysis of various selected simple models in the literature, in an effort to develop a flying ornithopter model. Further considerations will be given to other important parameters such as flapping frequency and wing geometry for well conceived formulations with realistic and workable assumptions and limitations.

© 2012 Elsevier B.V...Selection and peer-review under responsibility of Bin Nusantara University

Keywords: Unsteady Aerodynamics; Flapping Wing Aerodynamics; Micro-Air-Vehicle; Ornithopters

* Corresponding author. Tel.: +603-8956 6397; +6017-416 9045; fax: +603-8658 7125.
E-mail address: harijono@djojodihardjo.com.

1. Introduction

Human desire to mimic flying biosystems such as insects and birds through engineering to meet human needs has existed for hundreds of years and motivated mankind creativity, from Leonardo Da

Nomenclature

AR	aspect ratio	U	flight velocity
b	wingspan	V_x	velocity component along x-axis
c	chord	V_z	velocity component along z-axis
$C(k)$	Theodorsen function	V_T	tangential velocity to the section
$C_{d(f)}$	drag coefficient due to skin friction	V	relative velocity
C_{dp}	profile drag coefficient	w_0	downwash velocity at $3/4$ -chord location
C_{di}	induced drag coefficient	ρ	air density
C_{l-c}	lift coefficient for flat plate	β	flapping angle
C_l	lift coefficient	β_{max}	maximum flapping angle
C_n	normal force coefficient	β_p	stroke plane angle
dD_d	sectional total drag	$\dot{\beta}$	flapping rate
dD_f	sectional friction drag	$\ddot{\beta}$	flapping acceleration
dD_p	sectional profile drag	θ	pitching angle
dD_i	sectional induced drag	$\dot{\theta}$	pitching rate
dF_x	sectional chordwise force	$\ddot{\theta}$	pitching acceleration
dL	sectional instantaneous lift	θ_0	maximum pitch angle
dL_c	sectional lift	$\bar{\theta}_a$	angle of flapping axis with respect to stream velocity
	width of sectional strip under consideration	$\bar{\theta}_w$	mean angle of chord with respect to flapping axis
dN	sectional total attached flow normal force	$\bar{\theta}$	mean pitch angle
dN_c	sectional circulatory normal force	ϕ	lag between pitching and flapping angle
dN_{nc}	sectional apparent mass effect	δ	incidence angle
dT	sectional instantaneous thrust	γ	flight path angle
f	wingbeat frequency	ψ	relative angle between two velocity components
g	gravitational acceleration	α	relative angle of attack
\dot{h}	plunging rate	α_0	zero-lift angle
r	distance along the span of i th strip	η_s	efficiency coefficient
S	wing area		
t	time		

Vinci's drawings to Otto Lilienthal's gliders, to modern aircraft technologies and present flapping flight research. Two groups of flapping flight may be distinguished, bird flight and insect flight, each of which reveals different flight characteristics and capabilities. Perhaps the most comprehensive account of insect flight or entomopter to date is given by Ellington [1-3], Dickinson, Lehmann and Sane [4] and Ansari, Zbikowski and Knowles [5], while one of the first successful attempts to develop bird-like flapping flight was made by DeLaurier [6]. In the present work, a generic approach is followed to understand and mimic the unsteady aerodynamics of bio-inspired bird- or pterosaur-like flapping wing to produce lift and thrust for hovering and forward flight in an attempt to develop a simple and workable Micro-Air-Vehicle (MAV) ornithopter flight model, since such model does not need to generate more involved leading edge vortex and wake penetration exhibited by insect flight [1-3]. The use of a flexible membrane allows the wing to passively change its relative angle of attack

(AOA) and camber during the stroke cycle. This is the mechanism that has been utilized by operational commercially-available ornithopters.

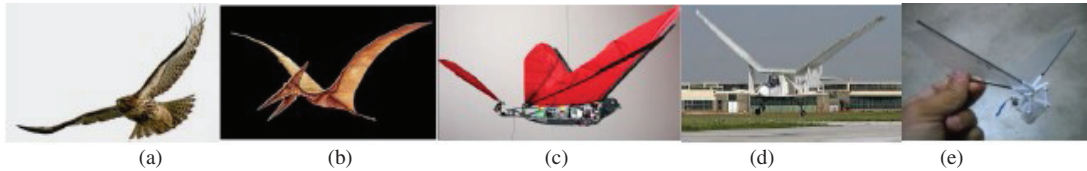


Figure 1: Modelling of Flapping Wing Ornithopter; (a) Flying Eagle; (b) Pterosaur [7]; (c) Jackowski completed Ornithopter [8]; (d) DeLaurier Ornithopter [9]; (e) A Flapping Wing Mock-up developed in a previous study [10].

The generic train of thought in modelling and developing up and down flapping motion configuration with flexible membrane wing skins can be summarized in Figure 1, to mimic the flapping wing mechanism of a real bird or pterosaur, exhibited in Figure 1(a) and (b), respectively. Such flapping mechanism and motion is also exhibited in a relatively small flying model of a flapping-wing ornithopter in Figure 1(c) [5], while Figure 1(d) exhibits a Flying Ornithopter-like Aircraft built by DeLaurier [4], while Figure 1(e) exhibits a simplified model for the flapping wing mechanism of such an ornithopter. The modelling of a simplified avian-based flight as represented by Figures 1(c)-(e) could be developed and substantiated using a simplified theoretical foundation as a baseline for understanding and developing more complicated Ornithopter autonomous flight. Following earlier work [11], Aerodynamic Strip theory and Theodorsen-Jones [12-13] unsteady aerodynamics will be utilized. Garrick leading-edge suction formulation [14-16] will also be utilized to investigate its influence. Reynolds number is a significant dimensionless aerodynamic parameter that characterizes ornithopter's flight as compared to high speed aircraft flights. For an airfoil with a 0.25 m chord length, an average size for the fixed wing UAV with a one meter span, the airfoil Reynolds numbers will be between 75,000 and 200,000 at cruise speeds of 10 to 30 km/hr. This Reynolds number range is a transition region with increasingly poor lift-to-drag ratios for smooth fixed wing airfoils [16]. Considerations will be given to oscillatory motion of the idealized wing in pitching and flapping with phase lag. By carrying out parametric study, the lift, drag, and thrust characteristics within a cycle for various configurations and operational parameters can be obtained, which could be considered for synthesizing proof-of-concept Flapping Wing MAV model with simplified mechanism. Computational code for the modelling of ornithopter unsteady aerodynamic is developed which can be further enriched with additional motion elements and control elements, and to synthesize a laboratory model.

2. Kinematics of Flapping Wing Motion

The flapping wing motion of ornithopters and entomopters can be generally grouped in three classes, based on the kinematics of the wing motion and mechanism of forces generation; the horizontal stroke plane, inclined stroke plane and vertical stroke plane [3]. The most distinctive characteristic in insect flight is the wing kinematics [5]. Due to smaller scale by nature, insects differ fundamentally from birds in which all actuations are carried out at the wing root. Unlike insect, birds have internal skeletons to which muscles are attached, enabling more localized actuation along the wing, for example, wing warping, although commonly, bird wing deflection may be passive. As a result from these kinematics, the aerodynamics associated with insect flight are also very different from those met in conventional fixed- and rotary-wing or even bird flight [5]. Based on Ellington's study [1-3], the kinematic of flight produced by the generic wing (semi-elliptical wing) can be

classified into the inclined stroke plane, where the resultant force produced by the wing can be separated into vertical and horizontal components, which are lift, thrust and drag, respectively throughout the up-stroke and down-stroke cycle; the inclined stroke plane, where a large horizontal thrust component will be produced (see Figure 2); and the vertical stroke plane, which is often seen during take off and hovering of butterflies and in which the wing motion is perpendicular to the chord. During flapping, the magnitude of the vertical induced flow is maximum near the wing tips and decreases as it approaches the root. Thus for constant forward speed, the relative angle of attack (AOA) also decreases from tip towards root. Figure 2 illustrates an inclined stroke plane during hovering flight prevailing during the wingbeat of the long-eared bat *Plecotus Auritus* [17].

To maintain low Angle of Attack (AOA) at the tip to meet attached flow situation, the wing must pitch in the direction of the flapping. During the down-stroke the total aerodynamic force is tilted

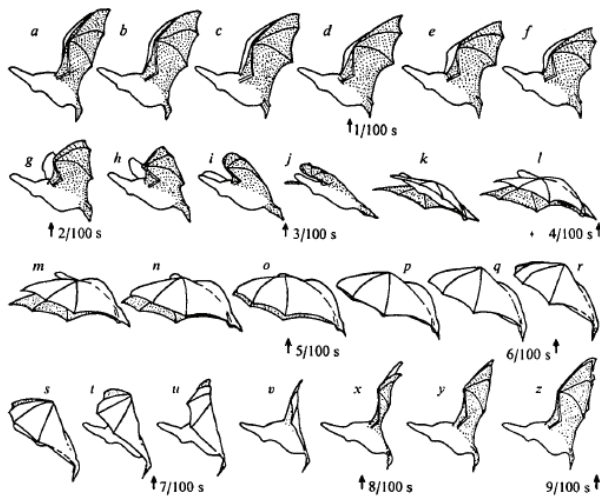


Figure 2: The wingbeat of the long-eared bat *Plecotus auritus*, illustrating an inclined stroke plane during hovering flight [17].

forward and has two components, lift and thrust. During the up-stroke, the AOA is always positive near the root but at the tip it can be positive or negative depending on the amount of pitching up of wing. Therefore, during up stroke the inner part of wing produces aerodynamic force which is upward but tilted backwards producing lift and negative thrust. The outer region of the wings would produce positive lift and drag if the AOA is positive. But if AOA is negative then it will produce negative lift but positive thrust [16]. In the kinematic modelling adopted in the present study of the flapping wing flight of pterosaur, only periodic flapping and pitching motions will be considered, and without losing generalities, the flapping axis is assumed to be very close to the body longitudinal axis and pitching motion axis at the

leading edge of the wing. This kinematic modelling is implied in Figure 5.

In the present development, some observations obtained by Pennycuik [18] will be considered. Using a combination of multiple regressions and a dimensional analysis, flight parameter for flapping flight can be correlated by geometrical characteristics of the flying birds and insects. Pennycuik experimentally derived the correlation of the wingbeat frequency for flapping flight to the body mass, wingspan, wing area and the wing moment of inertia. For birds with the body mass ranging from 20g to nearly 5kg the wingbeat frequency is correlated by the following formula:

$$f = \frac{1.08}{b} \sqrt[3]{\frac{m}{\rho}} \sqrt{\frac{g}{S}} \quad (1)$$

where m is the bird's body mass in kg, g is the gravitational acceleration, b is the wingspan, S is the wing area and ρ is the air density, which has been observed by Bunget [19] to give a good fit when

applied to small birds, bats and insects. In addition, the flight velocity mass can also be correlated to the mass of the bird or flying insect by (adapted from Pennycuik[18], Ho et al [21]):

$$U = 1.508(m)^{\frac{1}{6}} \quad (2)$$

3. Theoretical development of the Aerodynamics of Flapping Wings

Following the frame of thought elaborated in the previous section, several generic wing planforms are chosen in the present work as baseline geometries for the ornithopter wing Biomimicry Flapping Mechanism, among others the semi elliptical wing (shown in Figure 3) with the backdrop of various wing-planform geometries utilized by various researchers.

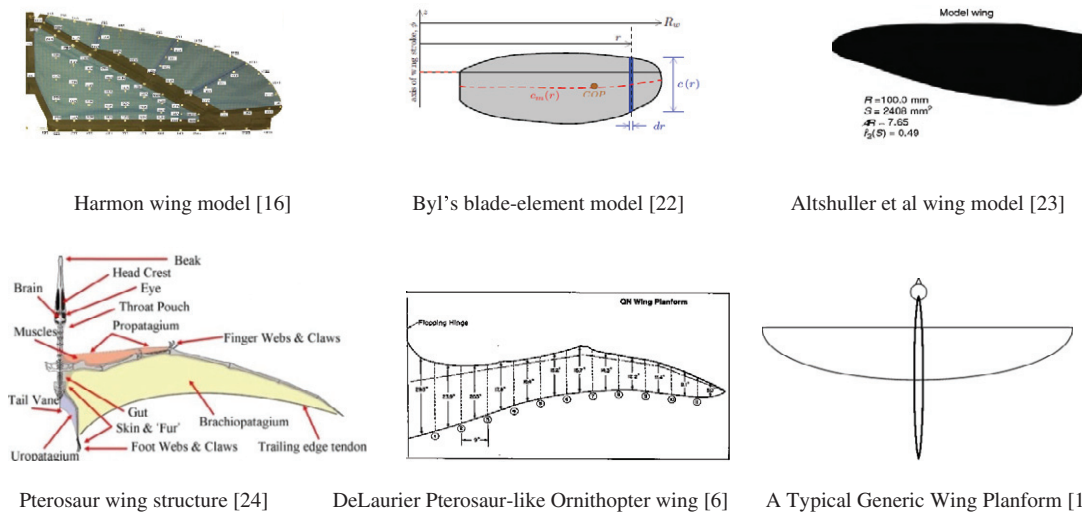


Figure 3: A generic semi-elliptical ornithopter's wing planform with the backdrop of various wing-planform geometries

The present work resorts to analytical approach to the flapping wing aerodynamic problem, which can be separated into quasi-steady and unsteady models. The quasi-steady model assumes that flapping frequencies are slow enough that shed wake effects are negligible, as in pterosaur and medium- to large-sized birds while the unsteady approach attempts to model the wake like hummingbird and insects. Smith et al [25] classifies the quasi-steady approaches to six techniques, which include momentum theory, blade element theory, hybrid momentum theory, lifting-line theory, thin-airfoil theory and lifting-surface theory.

Blade element theory has been utilized for flapping wing analysis by Ellington [3], DeLaurier [6], Byl [22] and Shyy [26]. In the present work, unsteady aerodynamics of a flapping wing using a modified strip theory approach is utilized as a simplification of DeLaurier's approach [6] for pterosaur flapping-wing aerodynamics. The lift, drag and thrust generated by pitching and flapping motion of three-dimensional rigid wing are computed using strip theory and Jones' modified Theodorsen approach without post-stall behaviour as a structured adaptation of DeLaurier's [6], Harmon [16], Byl's [22] and Malik et al's [27] procedures. Through such approach, a novel initiative is carried out for the parametric study on the contribution of wing pitching motion, flapping motion and coupled

motion, as well as the influence of pitch-flap phase lag for insight and optimization purposes by looking into the influence of the variation of the forward speed, flapping frequency and pitch-flap phase lag.

Two generic approaches are followed in the modelling of the aerodynamic calculation of the lift, drag and thrust generated by flapping wing motion. These are the computation of lift, drag and thrust generated by pitching and flapping motion of three-dimensional rigid wing using strip theory and Jones' modified Theodorsen approach which incorporate Garrick's leading edge suction without spanwise twist and post-stall behaviour as a simplified adaptation of DeLaurier's approach, and the computation of lift, drag and thrust generated by pitching and flapping motion of three-dimensional rigid wing in a structured procedure using strip theory and Jones' modified Theodorsen approach without camber, leading edge suction and post-stall behaviour.

The present study also addresses the contribution of wing pitching motion, flapping motion and coupled motion, as well as investigating the influence of pitch-flap phase lag, as a novel initiative, and parametric study for insight and optimization purposes by looking into the influence of the variation of the forward speed, flapping frequency and pitch-flap phase lag. The results of DeLaurier [6], Byl [22], Malik et al [27] and Zakaria et al [28] are used for validation. The computational logic in the present work is summarized in the Flow-Chart exhibited in Figure 4.

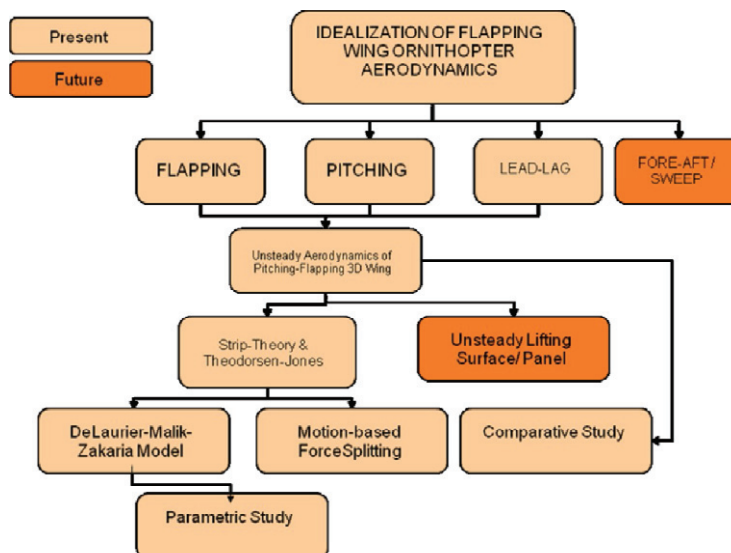


Figure 4: Ornithopter Flapping Wing Aerodynamics Computational Scheme

Present Work - First Procedure

This procedure basically follows pitching-flapping motion of rigid wing that is a structured adaptation and simplification of the procedure adopted by DeLaurier [6], Harmon [16], Malik et al. [27] and Zakaria et al [28]. The flapping wing can have three distinct motions with respect to three axes as: a) *Flapping*, which is up and down stroke motion of the wing, which produces the majority of the bird's power and has the largest degree of freedom. b) *Feathering* is the pitching motion of wing and can vary along the span. c) *Lead-lag*, which is in-plane lateral movement of wing.

Flapping angle β varies as sinusoidal function. β and its rate are given by following equations. The degree of freedom of the motion is depicted in Figure 5. Flapping angle β varies as sinusoidal function. The angle β and its rate and pitching angle θ are given by

$$\beta(t) = \beta_{\max} \cos 2\pi ft ; \quad \dot{\beta}(t) = -2\pi f \beta_{\max} \sin 2\pi ft ; \quad \theta(t) = \frac{r}{B} \theta_0 \cos(2\pi ft + \phi) \quad (3)$$

where θ_0 is the maximum pitch angle, ϕ is the lag between pitching and flapping angle and r is the distance along the span of the wing under consideration.

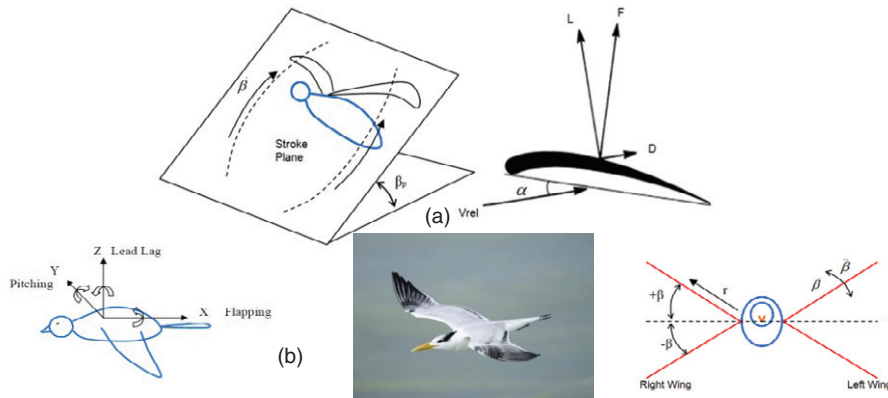


Figure 5: Angular movement of wing, adapted from Harmon [16]; stroke plane is indicated in (a), an adaptation of Ellington's configuration (where β_p is stroke plane angle) [3].

The vertical and horizontal components of relative wind velocity, as depicted in Figure 6, can be expressed as

$$V_x = U \cos \delta + (0.75 * c * \dot{\theta} * \sin \theta) \quad (4)$$

$$V_z = U \sin \delta + (-r * \dot{\beta} * \cos \beta) + (0.75 * c * \dot{\theta} * \sin \theta) \quad (5)$$

For horizontal flight, the flight path angle γ is zero. Also, $0.75 * c * \dot{\theta}$ is the relative air effect of pitching rate $\dot{\theta}$ which is manifested at 75% of the chord length [6].

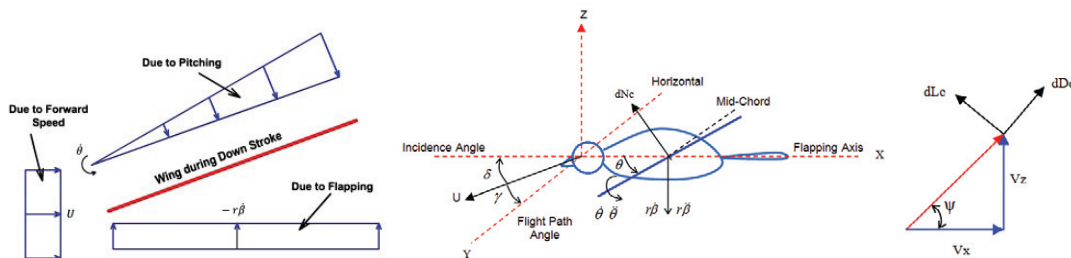


Figure 6: (a) Relative flow of air, adopted from [16]; (b) Forces on each section of the wing.

The relative velocity, relative angle between two velocity components ψ and the relative angle of attack can be expressed as

$$V = \sqrt{V_x^2 + V_z^2} \quad ; \psi = \tan^{-1} \left(\frac{V_z}{V_x} \right) \quad ; \text{ and } \quad \alpha = \psi + \theta \quad (6)$$

The section lift coefficient due to circulation (Kutta-Joukowski condition, flat plate) is given by [6]

$$C_{l-c} = 2\pi C(k) \sin \alpha \quad (7)$$

The sectional lift dL_c can then be calculated by

$$dL_c = \frac{1}{2} \rho V^2 C_{l-c} * c * dr \quad (8)$$

which should be integrated along the span to obtain the flapping-wing lift. Here c and dr are the chord length and width of the element of wing under consideration, respectively. The apparent mass effect (momentum transferred by accelerating air to the wing) for the section, is perpendicular to the wing, and acts at mid chord, and can be calculated as [15, 16]

$$dN_{nc} = -\frac{\rho \pi c^2}{4} (\dot{\theta} U + r \ddot{\beta} \cos \theta - 0.5 \ddot{\theta}) dr \quad (9)$$

The drag force has two components, profile drag dD_p and induced drag dD_i . These are calculated as

$$dD_p = \frac{1}{2} \rho V^2 C_{dp} * c * dr \quad (10)$$

$$dD_i = \frac{1}{2} \rho V^2 C_{di} * c * dr \quad (11)$$

where the values for the drag coefficients C_{dp} , C_f , C_{di} are assumed to be similar to those associated with basic geometrical cases (such as flat plate, airfoil with tabulated data and the like). C_f is the skin friction coefficient for flat plate and to account for profile drag, a factor K is introduced [15, 16]. A maximum value of K of 4.4 as given by Scherer [15] will be used. C_{di} is induced drag coefficient, and e is the efficiency factor of the wing and is 0.8 for elliptical wing. Total section drag is thus given by

$$dD_d = dD_p + dD_i \quad (12)$$

The circulatory lift dL_c , non-circulatory force dN_{nc} and drag dD_d for each section of the wing changes its direction at every instant during flapping. These forces in the vertical and horizontal directions will be resolved into those perpendicular and parallel to the forward velocity, respectively. The resulting vertical and horizontal components of the forces are given by

$$dF_{ver} = dL_c \cos \psi * \cos \delta + dN_{nc} \cos(-\theta) * \cos \beta * \cos \delta + dD_d \sin \psi * \cos \delta \quad (13)$$

$$dF_{hor} = dL_c \sin \psi * \cos \delta + dN_{nc} \sin(-\theta) * \cos \beta * \cos \delta - dD_d \cos \psi * \cos \delta \quad (14)$$

and are calculated within one complete cycle, and averaged to get the total average lift and thrust of the ornithopter.

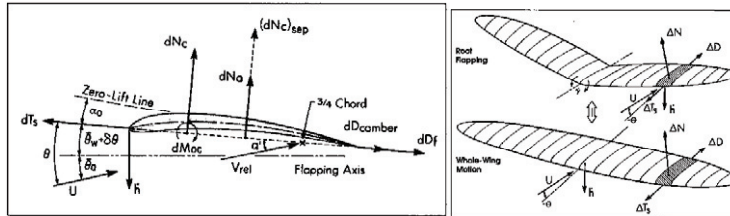


Figure 7: DeLaurier Ornithopter Model and Schematic [6].

Second Procedure

Under the more sophisticated consideration of DeLaurier Ornithopter model and schematic shown in Figure 7, where camber, downwash effect, leading edge suction and post-stall behaviour are included. The strip theory approach assumes that the aspect ratio of the wing is sufficiently large to allow the treatment of the flow over each section as essentially chordwise (in the free-stream direction). Therefore, the section's circulatory normal force is given by

$$dN_c = \frac{\rho UV}{2} C_n(r) cdr \quad (15)$$

V is flow's relative velocity at the $1/4$ -chord location, and the parameters in equation (15) are illustrated in Figure 7, where α_0 is the angle of the zero lift, and $\bar{\theta}$ is the section's mean pitch angle.

$$C_n(r) = 2\pi(\alpha' + \alpha_0 + \bar{\theta}) \quad (16); \quad \text{where } \bar{\theta} = \bar{\theta}_a + \bar{\theta}_w \quad (17)$$

where $\bar{\theta}_a$ is the angle of the flapping axis with respect to the free- or mean-stream velocity, U , and $\bar{\theta}_w$ is the mean angle of the chord with respect to the flapping axis. As depicted in Figure 7, in equation (15), α' is given by

$$\alpha' = \left[\frac{AR * C(k)}{(2 + AR)} \right] \alpha - \frac{w_0}{U} \quad \left(\text{where } \frac{w_0}{U} \text{ is the downwash term [6].} \right) \quad (18)$$

The relative angle of attack α at the $3/4$ -chord location due to the wing's motion is given by

$$\alpha = \frac{\left(\dot{h} \cos(\theta - \bar{\theta}_a) + \frac{3}{4} c \dot{\theta} + U(\theta - \bar{\theta}) \right)}{U} \quad (19)$$

where $C'(k)$, $F'(k)$ and $G'(k)$ relate to the well known Theodorsen function [12] which are functions of reduced frequency k . Garrick's [14] expression for the leading edge suction of two dimensional airfoil is applied to the present strip theory model by combining it with equation (18) to yield

$$dT_s = \eta_s 2\pi \left(\alpha' + \bar{\theta} - \frac{1}{4} \frac{c\dot{\theta}}{U} \right)^2 \frac{\rho UV}{2} c dr \quad (20)$$

The efficiency term η_s accounts for viscous effect on the potential-flow theory leading edge suction. The chordwise friction drag and the flow speed tangential to the section V_T are given by

$$dD_f = (C_d)_f \frac{\rho V_T^2}{2} c dr \quad (21); \quad V_T = U \cos \theta - \dot{h} \sin(\theta - \bar{\theta}_a) \quad (22)$$

$(C_d)_f$ is the drag coefficient due to skin friction. Thus, the total chordwise force is

$$dF_x = dT_s - dD_{camber} - dD_f \quad (23)$$

The instantaneous lift and thrust are then given by:

$$dL = dN \cos \theta + dF_x \sin \theta \quad (24)$$

$$dT = dF_x \cos \theta - dN \sin \theta \quad (25)$$

which can be integrated along the span to give the instantaneous lift and thrust of the wing. For n strips of equal width and one flap cycle with m equal time steps, the average lift, thrust and drag can readily be calculated by numerical integration.

4. Results and Analysis

The results below are obtained using the following wing geometry and parameters: the wingspan 40cm, aspect ratio 6.2, flapping frequency 7Hz, total flapping angle 60° , forward speed 6m/s, maximum pitching angle 20° , and incidence angle 6° . The computational scheme developed has been validated satisfactorily.

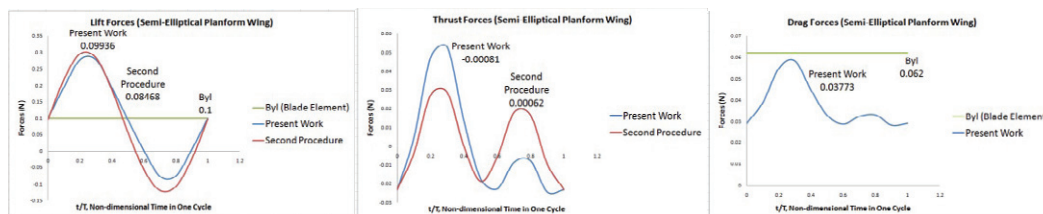


Figure 8: Lift and Thrust Forces (and Drag Force for the Present Work) with Rectangular Planform Wing; (a) Present Work; (b) Second Procedure (in a companion paper, in progress).

A sample of such validation is shown in Figures 8, 9 and 10. To gain some insight on how these computational models compare with the biosystems to mimic, Table 1 is prepared to exhibit the ratio of the lift per cycle calculated using the Present Work and those obtained by other investigators; for comparison, the weight per wing-span of a selected sample of birds are also exhibited. Although the

comparison is by no means rigorous, it may shed some light on how the geometrical modelling and the flapping motion considered in the computational model may contribute to the total lift produced and how further refinement could be synthesized.

Figure 8 was obtained using aerodynamic strip theory and Theodorsen-Jones modified formulations, where the geometry is similar to Harmon's and the parameters are relatively close to Harmon's. The following assumptions were made: the pitching and flapping motions are in sinusoidal motion, and the upstroke and downstroke phases have equal time duration. There is incidence angle, which is 6° and there is no flight path angle.

The phase lag was assumed to be fixed at 90° . Harmon's example [16] did not incorporate the leading edge suction, wake capture and dynamic stall. As Figure 9 indicates, the computational results using the present second generic method have comparable agreement to the measured results by Harmon (indicated by the blue line in his work).

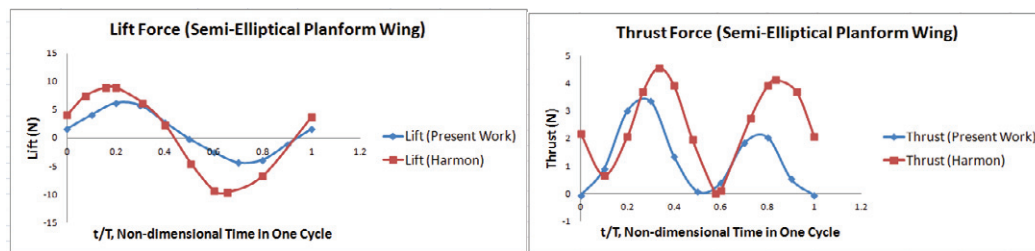


Figure 9: Comparisons of the results of the Present Work with Harmon's [16] for similar wing planforms.

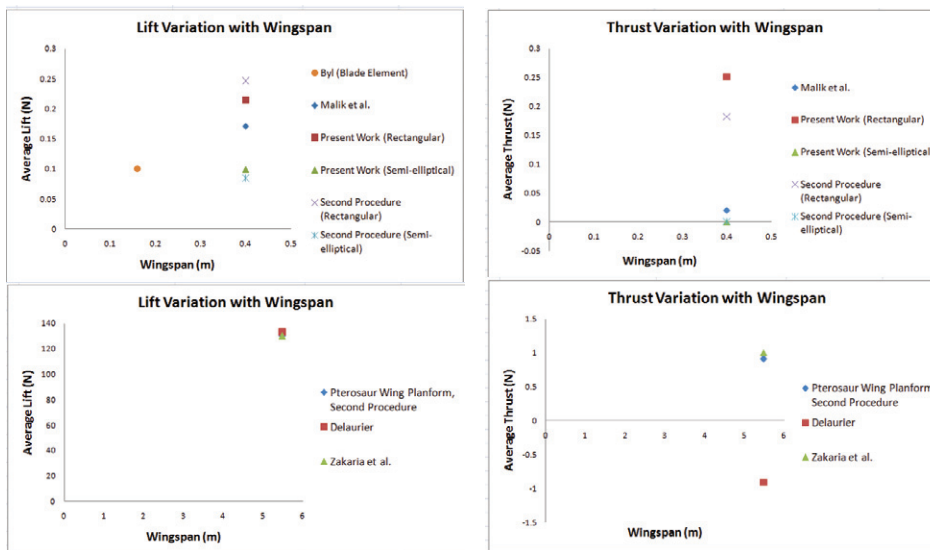
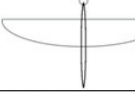
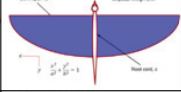
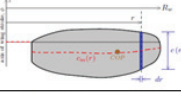
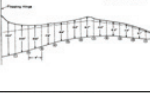






Figure 10: Comparisons of the results of the Present Work and Second Procedure (in a companion paper, in progress) with Malik et al's [27] for both rectangular and semi-elliptical wing planforms.

Table 1: Comparison of basic performance of ornithopter models and birds

Source: <http://www.nwf.org/wildlife/activities/national-wildlife-week/-/media/5B8F83ED421542B794D1396475C450CD.ashx>

ORNITHOPTER MODEL	First Procedure	Malik et al	Byl's hummingbird-scale robot	DeLaurier pterosaur model
Length	-			
Wingspan	0.4m	0.4m	0.16m	5.4864m
Average Lift/Cycle	0.099361N	0.1705N	0.1N	133N
				
$ratio(N/m) = \frac{Lift(N)}{Wingspan(m)}$	0.2484N/m	0.4263N/m	0.6250N/m	24.2418N/m
BIRD	Turkey Vulture	Red-tailed Hawk	Bald Eagle	Peregrine Falcon
Length	67 cm (26 in)	49 cm (19 in)	79 cm (31 in)	46 cm (18 in)
Wingspan	171 cm (67 in)	125 cm (49 in)	203 cm (80 in)	116 cm (46 in)
Mass	1.8 kg (4 lb)	1.082 kg (2.4 lb)	4.3 kg (9.5 lb)	0.952kg (2.1 lb)
				
$ratio(N/m) = \frac{Lift(N)}{Wingspan(m)}$	$\frac{18(N)}{1.71(m)} = 10.5$	$\frac{10.82(N)}{1.25(m)} = 8.656$	$\frac{43(N)}{2.03(m)} = 21.182$	$\frac{9.52(N)}{1.16(m)} = 8.206$
Wing Area following Tucker's Formula [30]	0.425 m ² *	0.305 m ² *	0.639 m ² **	0.149 m ² ***
Wing beat Frequency	2.79 Hz	3.50 Hz	2.84 Hz	4.32 Hz

Applicable Tucker's formula: *(S=0.260b-0.020), **(S=0.335b-0.041), ***(S=0.112b+0.019).

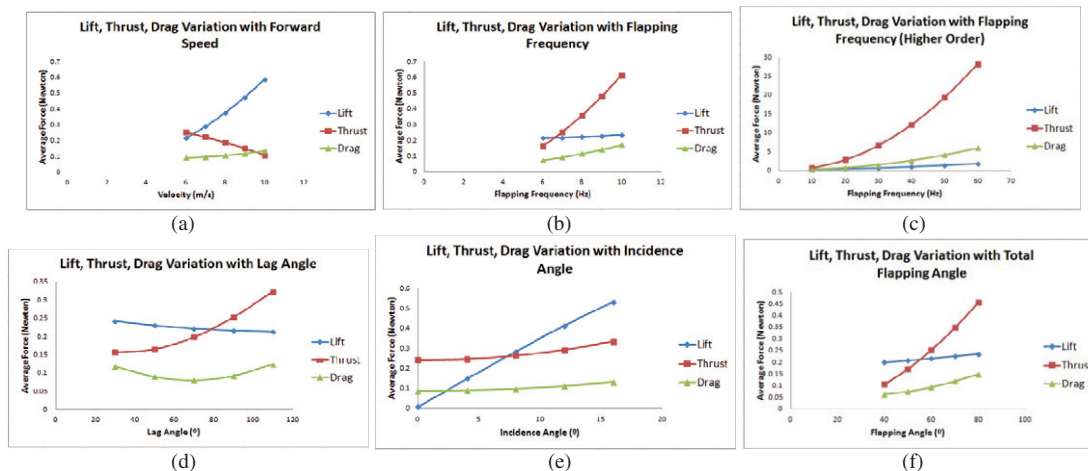


Figure 11: Parametric Study on the influence of forward speed (a), flapping frequency (b, c), flapping-pitching phase lag (d), angle of incidence (e) and total flapping angle (f) on cyclic lift, drag and thrust (for a wing of rectangular planform).

Parametric study

A parametric study is carried out to assess the influence of some flapping wing motion parameters to the flight performance desired. The study considers the following parameters: the Effect of Forward speed, the Effect of Flapping Frequency, the Effect of Lag Angle, the Effect of Angle of Incidence and the Effect of Total Flapping Angle. The results are exhibited in Figure 11. An interesting result is exhibited by Figure 11 (b) and (c), where the wingbeat frequency has been varied and the thrust is consistently increased with the increase of the wingbeat frequency, while the lift increases only slightly. If reference is made to Pennycuick's formula (1) and Tucker's formula [30] to correlate wing-

span and wing area of birds, the present ornithopter model operating frequencies as anticipated in Figure 11 are close to the operating flapping frequency values of selected birds shown in Table 1.

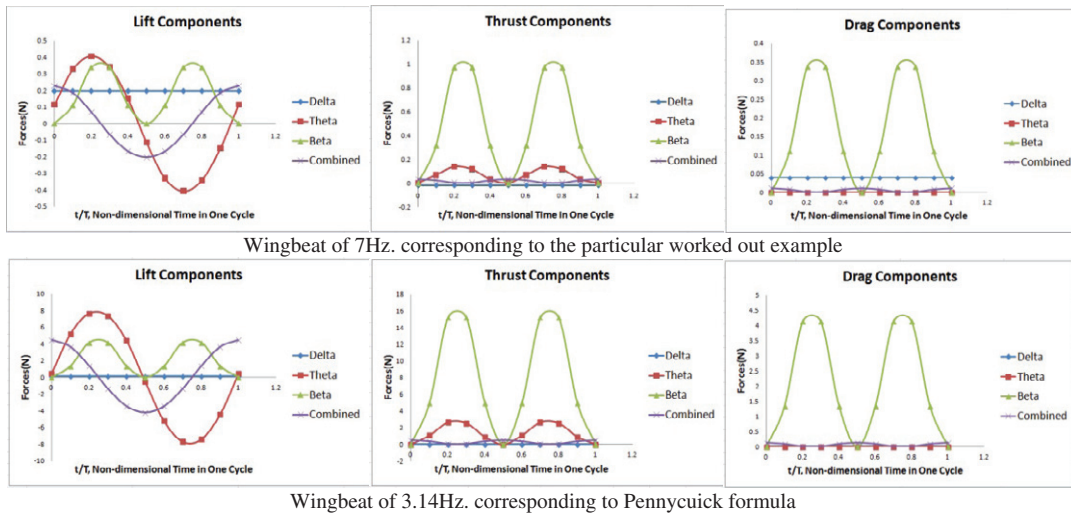


Figure 12: The influence of individual contributions of the pitching-flapping motion and their phase lag on the flight performance. The influence of the flapping frequency is consistent as illustrated in Figure 11.

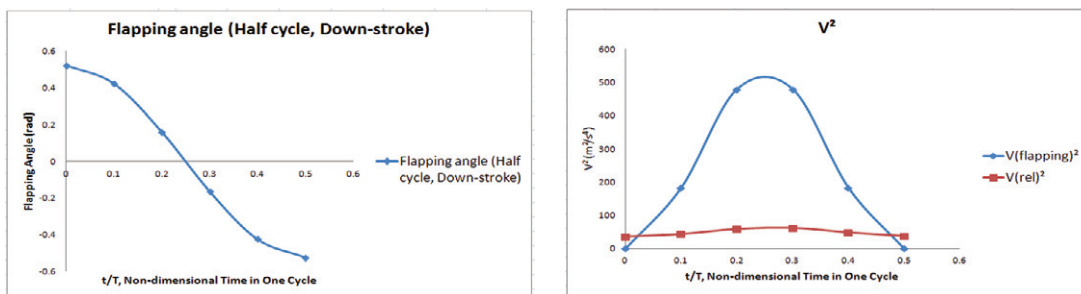


Figure 13: Verification of the observation of Ellington et al [3] on the notion that the value of V_{rel}^2 is well below V_{flapping}^2 using the present simple modelling.

Motion Based Forces Splitting

Another study is carried out to investigate the influence of individual contributions of the pitching-flapping motion and their phase lag on the flight performance. The calculation is performed on rectangular wing. Results obtained as exhibited in Figure 12 show that for the lift, the pitching angle dominates the force, while for the thrust, the flapping angle. The drag is also dominated by flapping effect.

Verification of the present kinematic and aerodynamic modelling of flapping motion

The relative velocity, V_{rel} on the downstroke should not be approximated by the flapping velocity, V_{flapping} [3]. Due to the inclination of the stroke plane, the induced velocity will reduce the value of V_{rel}^2 well below V_{flapping}^2 . An accurate estimate of the induced velocity is therefore essential in

calculating the magnitude and direction of the relative velocity [3]. The present modelling, as exhibited in Figure 13, verifies such state of affairs.

5. Conclusions

The present work has been performed to assess the effect of flapping-pitching motion with pitch-flap phase lag in the flight of ornithopter. In this conjunction, a computational model has been considered, and a generic computational procedure has been adopted. Two-dimensional unsteady theory of Theodorsen with modifications to account for three-dimensional and viscous effects, leading edge suction and post-stall behaviour. The study is carried out on rectangular and semi-elliptical wing planforms. The results have been compared and validated with others within similar unsteady aerodynamic approach and general physical data, and within the physical assumptions limitations, have encouraging qualitative agreement or better. Judging from lift per unit span, the present flapping-wing model performance is comparable to those studied by Byl [22] and Malik et al [27], while DeLaurier's pterosaur model [6] is order of magnitude larger and comparable to Bald Eagle.

The analysis and simulation by splitting the flapping and pitching motion shows that: (a) The lift is dominantly produced by the pitching motion, since the relative airflow effect prevailed along 75% of the chord length. (b) The thrust is dominated by flapping motion. The vertical component of relative velocity increases significantly as compared to the horizontal components, which causes the force vector produced by the flapping-pitching motion to be directed towards the horizontal axis (thrust axis). (c) The drag is dominated by the flapping motion, due to higher relative velocity as well as higher induced drag due to circulation.

A structured approach has been followed to assess the effect of different design parameters on lift, thrust, and drag of an ornithopter, as well as the individual contribution of the component of motion. These results lend support to the utilization of the generic modelling adopted in the synthesis of a flight model, although more refined approach should be developed. Various approaches for ornithopter aerodynamic modelling could be followed, such as the incorporation of other parameters, and the use of more refined blade element, CFD or lifting surface methods. In retrospect, a generic physical and computational model based on simple kinematics and basic aerodynamics of a flapping-wing ornithopter has been demonstrated to be capable of revealing its basic characteristics and can be utilized for further development of a flapping-wing MAV.

Acknowledgement

The authors would like to thank Universiti Putra Malaysia (UPM) for granting Research University Grant Scheme (RUGS) No. 05-02-10-0928RU; CC-91933, under which the present research is carried out.

References

- [1]. Ellington, C.P., *The Aerodynamics of Hovering Insect Flight*, III. Kinematics – 1984, *Phil. Trans. R. Soc. Lond. B* 1984 **305**, 41-78, rsta.royalsocietypublishing.org/content/305/1122/41.short
- [2]. Ellington, C.P., The Novel Aerodynamics of Insect Flight: Applications to Micro-Air Vehicles, *The Journal of Experimental Biology* 202, 3439–3448 (1999)

- [3]. Ellington, C.P., The Aerodynamics of Hovering Insect Flight, I, Quasi-Steady Analysis, Phil.Trans.of Roy.Soc.London, B, Bio.Sci., Vol 35, No 1122, Feb 1984
- [4]. Dickinson, M.H., Lehmann, F.O. and Sane, S.P., Wing Rotation and the Aerodynamic Basis of Insect Flight, *Science* 284, 1954 (1999);
- [5]. Ansari, S.A., Zbikowski, R. and Knowles, K., Aerodynamic modelling of insect-like flapping flight for micro air vehicles, *Progress in Aerospace Sciences* 42 (2006) 129–172.
- [6]. DeLaurier, J.D., An Aerodynamic Model for Flapping Wing Flight. *The Aeronautical Journal of the Royal Aeronautical Society*, April 1993, pp. 125-130.
- [7]. Strang, K.A., Efficient Flapping Flight of Pterosaurs, PhD, Stanford, 2009
- [8]. Jackowski, Z.J., Design & Construction of an Autonomous Ornithopter, MIT SB Thesis, 2009.
- [9]. <http://www.picsearch.com.vn/pictures/.com-EN/Vehicles/Aircrafts/xxx/pictures/.com-EN/Vehicles/Aircrafts/Aircrafts/20D/deLaurier/202001/20Ornithopter.html>
- [10]. Ramli, A.S.S., Aerodynamic Study and Conceptual Design of Flapping Wing Ornithopter, Bachelor Thesis, supervised by Harijono Djojodihardjo, Universiti Putra Malaysia, 2011.
- [11]. Djojodihardjo, H and Ramli, A.S.S., Generic and Parametric Study of the Aerodynamic Characteristics of Flapping Wing Micro-Air-Vehicle, AEROTECH IV paper, to be published by *Trans Tech Publications, Switzerland, 2012*
- [12]. Theodorsen, General Theory of Aerodynamic Instability and the Mechanism of Flutter.
- [13]. Jones, R.T, The unsteady lift of a wing of finite aspect ratio, NACA Report 681, 1940.
- [14]. Garrick, I.E., Propulsion of a Flapping and Oscillating Aerofoil, NACA Report No.567, 1936.
- [15]. Scherer, J.O., “Experimental and Theoretical Investigation of Large Amplitude Oscillating Foil Propulsion Systems”, Hydronautics, Laurel, Md, December 1968.
- [16]. Harmon, R.L., Aerodynamic Modelling of a Flapping Membrane Wing Using Motion Tracking Experiments. *Master's Thesis 2008, University of Maryland, 2008.*
- [17]. Norberg, U.M., Hovering Flight of *Plecotus auritus*, L. *Bijdr. Dierk* 40, 62-66 (Proc.2nd int. Bat.Res. Conf.), 1970.
- [18]. Pennycuik C J 1990 Predicting Wingbeat Frequency and Wavelength of Birds *The Journal of Experimental Biology* **150** 171 – 85
- [19]. Bunget, G., BATMAV – A Bio-Inspired Micro-Aerial Vehicle for Flapping Flight PhD, North Carolina, 2010
- [20]. Mueller, T.J., *Fixed and Flapping Wing Aerodynamics for Micro Air Vehicle Applications*. Reston, VA: AIAA, 2001.
- [21]. Ho, S., Nassef, H., Pornsinsirak, N., Tai, Y-C., Ho, C-M., Unsteady aerodynamics and flow control for flapping wing flyers, *Progress in Aerospace Sciences* 39 (2003) 635–681
- [22]. Byl, K., A passive dynamic approach for flapping wing micro aerial vehicle control, ASME Dynamic Systems and Controls Conference, 2010, http://www.ece.ucsb.edu/~katiebyl/papers/Byl10_DSCC.pdf, accessed 8 May 2012
- [23]. Altshuler, D.L., Dudley, R. and Ellington, C.P., Aerodynamic forces of revolving hummingbird wings and wing models, *J. Zool. Land.* (2004) 264, 327-332 © 2004.
- [24]. Strang, K.A., Efficient Flapping Flight of Pterosaur, PhD Thesis, Stanford University, 2009.
- [25]. Smith, M.J.C., Wilkin P.J., Williams, M.H., “The advantages of an unsteady panel method in modelling the aerodynamic forces on rigid flapping wings,” *The Journal of Experimental Biology*, Vol. 199, 1996, pp. 1073-1083.
- [26]. Shyy, W., Lian, Y., Tang, J., Vlieru, D., Liu, H., *Aerodynamics of Low Reynolds Number Flyers*. Cambridge University Press, New York, NY, 2008.
- [27]. Malik, M.A., Ahmad, F. (June 30-July 2, 2010). Effect of Different Design Parameters on Lift, Thrust, and Drag of an Ornithopter. *Proceedings of the World Congress on Engineering 2010 Vol II (WCE 2010)*, London, U.K.
- [28]. Zakaria, M. Y., Elshabka, A. M., Bayoumy, A. M., Abd Elhamid, O. E., Numerical Aerodynamic Characteristics of Flapping Wings, 13th International Conference on Aerospace Sciences & Aviation Technology, ASAT- 13, May 26 – 28, 2009
- [29]. <http://www.amazon.com/Foundations-Aerodynamics-Arnold-M-Kuethe/dp/0471509531>, A.M., Schetzer, J.D. and Chow, C-Y-, *Foundations of Aerodynamics*, John Wiley, 1976
- [30]. Tucker, V.A., Gliding Birds: The Effect Of Variable Wing Span, *J.Exp.Biology*, 133, 1987